International Journal of Medical Microbiology 309 (2019) 151355

Contents lists available at ScienceDirect

International Journal of Medical Microbiology

journal homepage: www.elsevier.com/locate/ijmm

Staphylococcus petrasii diagnostics and its pathogenic potential enhanced by mobile genetic elements

Veronika Vrbovská[a], Vojtěch Kovařovic[a], Ivana Mašlaňová[a], Adéla Indráková[a], Petr Petráš[b], Ondrej Šedo[c], Pavel Švec[d], Lenka Fišarová[a], Marta Šiborová[c], Kamil Mikulášek[c,e], Ivo Sedláček[d], Jiří Doškař[a], Roman Pantůček[a,*]

[a] Division of Genetics and Molecular Biology, Department of Experimental Biology, Faculty of Science, Masaryk University, Kotlářská 2, 611 37 Brno, Czech Republic
[b] Reference Laboratory for Staphylococci, National Institute of Public Health, Šrobárova 48, 100 42 Praha 10, Czech Republic
[c] Central European Institute of Technology, Masaryk University, Kamenice 5, 625 00 Brno, Czech Republic
[d] Czech Collection of Microorganisms, Department of Experimental Biology, Faculty of Science, Masaryk University, Kamenice 5, 625 00 Brno, Czech Republic
[e] National Centre for Biomolecular Research, Masaryk University, Kamenice 5, 625 00 Brno, Czech Republic

ARTICLE INFO

Keywords:
Coagulase-negative staphylococci
Mobile genetic elements
Methicillin resistance
MALDI-TOF MS
Molecular subtyping
Virulence factors

ABSTRACT

Staphylococcus petrasii is recently described coagulase negative staphylococcal species and an opportunistic human pathogen, still often misidentified in clinical specimens. Four subspecies are distinguished in *S. petrasii* by polyphasic taxonomical analyses, however a comparative study has still not been done on the majority of isolates and their genome properties have not yet been thoroughly analysed. Here, we describe the phenotypic and genotypic characteristics of 65 isolates and the results of *de novo* sequencing, whole genome assembly and annotation of draft genomes of five strains. The strains were identified by MALDI-TOF mass spectrometry to the species level and the majority of the strains were identified to the subspecies level by fingerprinting methods, $(GTG)_5$ repetitive PCR and ribotyping. Macrorestriction profiling by pulsed-field gel electrophoresis was confirmed to be a suitable strain typing method. Comparative genomics revealed the presence of new mobile genetic elements carrying antimicrobial resistance factors such as staphylococcal cassette chromosome (SCC) *mec*, transposones, phage-inducible genomic islands, and plasmids. Their mosaic structure and similarity across coagulase-negative staphylococci and *Staphylococcus aureus* suggest the possible exchange of these elements. Numerous putative virulence factors such as adhesins, autolysins, exoenzymes, capsule formation genes, immunomodulators, the phage-associated *sasX* gene, and SCC-associated spermidine N-acetyltransferase gene, pseudouridine and sorbitol utilization operons might explain clinical manifestations of *S. petrasii* isolates. The increasing recovery of *S. petrasii* isolates from human clinical material, the multi-drug resistance including methicillin resistance of *S. petrasii* subsp. *jettensis* strains, and virulence factors homologous to other pathogenic staphylococci demonstrate the importance of the species in human disease.

1. Introduction

Coagulase-negative staphylococci (CoNS) are considered to be typical opportunists (Heilmann et al., 2019), having a substantial impact on human life and health, particularly in immunocompromised patients (Becker et al., 2014). Antibiotic resistance has been documented to be more common in CoNS than in *S. aureus* (Brzychczy-Wloch et al., 2013; Otto, 2013). Developments in diagnostics have led to the frequent detection of *Staphylococcus petrasii* in human specimens and suggested that it is a clinically relevant species. Based on genotypic and phenotypic analyses, four subspecies *S. petrasii* subsp. *petrasii*, *S. petrasii* subsp. *jettensis*, *S. petrasii* subsp. *croceilyticus* and *S. petrasii* subsp. *pragensis* were described (De Bel et al., 2014, 2013; Pantucek et al., 2013; Svec et al., 2015). *S. petrasii* belongs to a phylogenetic clade including *Staphylococcus haemolyticus* and *Staphylococcus hominis* (Pantucek et al., 2013). The well-studied and phylogenetically related *S. haemolyticus* is known for its historically early acquisition of resistance to methicillin and glycopeptide antibiotics (Froggatt et al., 1989). It is possible that *S. haemolyticus* played an important role in the diversification of staphylococcal cassette chromosome *mec* (SCC*mec*) (Cavanagh et al., 2014; Zong et al., 2011), which led to an alarming prevalence of methicillin-resistant *S. haemolyticus* clinical isolates (Bouchami et al., 2012; Panda

* Corresponding author at: Department of Experimental Biology, Faculty of Science, Masaryk University, Kamenice 5, 625 00 Brno, Czech Republic.
E-mail address: pantucek@sci.muni.cz (R. Pantůček).

https://doi.org/10.1016/j.ijmm.2019.151355
Received 5 June 2019; Received in revised form 29 August 2019; Accepted 4 September 2019

et al., 2016). In contrast, SCC of *S. hominis* exhibited a limited clonality and a low genetic diversity (Bouchami et al., 2011). The properties of both species confirm they are significant opportunistic human pathogens (Barros et al., 2012; Chaves et al., 2005).

Although *S. petrasii* was described 6 years ago (Pantucek et al., 2013), there is limited knowledge of its pathogenicity, genome structure, mobile genetic elements (MGE) carrying virulence and drug resistance genes, and systems limiting the spread of these elements. A set of sixty-five strains originating from human clinical material was analysed in this study with a focus on improving *S. petrasii* diagnostics and the description of the species' diversity. Whole genomes of type strains of four *S. petrasii* subspecies and one additional methicillin-resistant isolate were sequenced and characterized in detail for a better understanding of its pathogenic potential.

2. Materials and methods

2.1. Bacterial strains

S. petrasii strains were collected from a set of CoNS referred by routine clinical laboratories for identification to the National Reference Laboratory for Staphylococci, National Institute of Public Health (NRL/St) (Prague, Czech Republic) as clinically significant agents isolated from clinical materials and from previous taxonomic studies (Table S1, Fig. S1) (De Bel et al., 2013; Pantucek et al., 2013; Svec et al., 2015). The possibility that strains were skin contaminants was excluded by disinfection before the blood collection and analysis of patients' skin microflora. Reference strains are available in the Czech Collection of Microorganisms (CCM) at Masaryk University (Brno, Czech Republic). The phenotypic identification of the isolates was done using commercial identification kits STAPHYtest 24 with ErbaExpert software (Erba Lachema, Brno, Czech Republic) and API Staph (bioMérieux, Marcy l'Etoile, France) according to the manufacturers' instructions.

2.2. Matrix-assisted laser-desorption/ionization time-of-flight mass spectrometry (MALDI-TOF MS) analysis

The samples were prepared by the standard extraction protocol described in detail by Freiwald and Sauer (Freiwald and Sauer, 2009). MALDI-TOF mass spectra were obtained using an UltrafleXtreme instrument (Bruker Daltonics, Bremen, Germany) operated in linear positive mode using the software FlexControl version 3.4. Signals present in at least seven out of nine independent mass spectra acquired per sample were taken into account. Mass spectra were processed using FlexAnalysis (version 3.4; Bruker Daltonics) and BioTyper software (version 3.1; Bruker Daltonics) supplemented with database version 8.0.0.0 (7854 entries). The mutual similarity between individual mass spectra of the strains and the Biotyper database entries were expressed in the form of log(scores) obtained using the default settings of the Biotyper software.

2.3. Genotypic analysis by fingerprinting techniques

Repetitive PCR fingerprinting with the $(GTG)_5$ primer ($(GTG)_5$-REP-PCR) was performed as described previously (Svec et al., 2010). The automatic ribotyping was performed using the RiboPrinter Microbial Characterization System (DuPont Qualicon, Wilmington, DE) in accordance with the manufacturer's instructions. Numerical analysis of the obtained fingerprints and dendrogram construction was done using the software BioNumerics version 7.6 (Applied Maths, Kortrijk, Belgium) and compared to the in-house CCM database of reference strains. The ribotype patterns were imported into BioNumerics using the load samples import script provided by the manufacturer.

Macrorestriction analysis with *Sma*I (New England BioLabs, Ipswich, MA) resolved by pulsed-field gel electrophoresis (PFGE) was performed as described previously (Pantucek et al., 1996). PFGE was done using a CHEF-Mapper system (Biorad, Hercules, CA) with 1.2% agarose gel (Serva, Heidelberg, Germany) in 1× Tris-acetate-EDTA (TAE) buffer for 20 h at 14 °C. Pulse times of 2 s to 12 s for 14 h at 5.5 V and 30 s to 45 s for 6 h at 6 V were used. The strain *S. petrasii* subsp. *petrasii* CCM 8418^T was used as a reference every sixth line of each gel. The gels were stained in 0.3% ethidium bromide for 3 h and photographed under UV light. Digital images were stored electronically as TIFF files and analyzed with BioNumerics version 7.6 software. Dendrograms were constructed using the Dice similarity coefficient (with 0.5% tolerance and 0.5% optimization) and the unweighted pair group method with arithmetic averages (UPGMA) for clustering.

2.4. Antimicrobial susceptibility tests

The antibiotic resistance was tested by the disc diffusion method on Mueller-Hinton agar (Oxoid, Basingstoke, UK) using seventeen antibiotics generally used for Gram-positive cocci (Oxoid): cefoxitin (30 µg), ciprofloxacin (5 µg), clindamycin (2 µg), erythromycin (15 µg), co-trimoxazole (25 µg), fusidic acid (10 µg), gentamicin (10 µg), rifampicin (5 µg), tigecycline (15 µg), mupirocin (5 µg), tetracycline (30 µg), chloramphenicol (30 µg), linezolid (10 µg), benzylpenicillin (1U), teicoplanin (30 µg), vancomycin (30 µg), and ceftaroline (5 µg). The incubation conditions were 16–20 h at 36 °C in air. EUCAST/CLSI standards for reading the inhibition zone diameter and interpreting susceptibility to antibiotics were strictly followed (CLSI, 2018; EUCAST, 2017). The presence of the methicillin resistance genes *mecA*, *mecB* and *mecC* was examined by PCR amplification with the primers SAMECA165 and SAMECA1482 for *mecA* (Wu et al., 1998), $mecA_{LGA251}$MultiFP and $mecA_{LGA251}$MultiRP for *mecC* (Stegger et al., 2012), and mecB-F (GGGACTATAGACGCATCAAC) and mecB-R (CCA GTAACTACTTTTCTCATGC) designed in this study for *mecB* gene.

2.5. rpoB gene sequencing

Partial *rpoB* gene amplification was performed as described previously (Mellmann et al., 2006). PCR amplicons were sequenced by Sanger sequencing with the primers 1418F and 1876R in Eurofins Genomics (Ebersberg, Germany). Phylogenetic analyses were performed with the software MEGA version 7 (Kumar et al., 2016).

2.6. Plasmid profiling

The plasmid DNA was extracted using a NucleoSpin© Plasmid Kit (Macherey-Nagel, Düren, Germany) according to the manufacturer's protocol with the modification that bacteria were lysed with 30 µg/ml of lysostaphin (Ambi Products, Lawrence, NY) at 37 °C. Undigested plasmid DNA was separated by agarose gel electrophoresis as described previously (Kuntova et al., 2012).

2.7. Genome sequencing and assembly

Genomic DNA was isolated and whole genomic sequencing was performed using an Ion Torrent™ Personal Genome Machine (Thermo Fisher Scientific, Carlsbad, CA). The purified genomic DNA was used for preparing a 400-bp sequencing library with an Ion Plus Fragment Library Kit (Thermo Fisher Scientific) as described previously (Pantucek et al., 2018). The sample was loaded onto a 318v2 chip and sequenced using an Ion PGM Hi-Q sequencing kit (Thermo Fisher Scientific). Quality trimming of the reads were performed with the Ion Torrent Suite Software version 5.0.4 with default settings. The assembly computation and error correction was performed using the assembler SPAdes version 3.11.1 pipeline (Nurk et al., 2013) with parameters adjusted for Ion Torrent data. Contigs were then re-ordered according to the reference genome *S. haemolyticus* JCSC1435 (Takeuchi et al., 2005) using MauveContigMover (Rissman et al., 2009). Ordering was evaluated using an assembly graph visualized in Bandage (Wick et al.,

2015). Plasmid contigs were extracted from WGS data based on higher coverage and content of typical plasmid-borne genes.

2.8. Bioinformatics analyses

Sequences were manipulated and inspected in the cross-platform bioinformatics software Ugene version 1.28.0 (Okonechnikov et al., 2012). For primary analysis, the genome was annotated using RAST (Aziz et al., 2008). Predicted protein sequences were clustered using web-based OrthoVenn with a default cutoff e-value of $1e^{-5}$ and an inflation value of 1.5 (Wang et al., 2015). Functional genome annotation was further performed using several databases; the NCBI BLAST service (blast.ncbi.nlm.nih.gov/Blast.cgi) and InterProScan (Jones et al., 2014). MGE were predicted using IslandViewer 4 (Dhillon et al., 2015), CRISPRone (Zhang and Ye, 2017), VIRFAM (Lopes et al., 2014) and ISfinder (Siguier et al., 2006). Antibiotic resistance determinants were screened with ResFinder (Zankari et al., 2012) and the RGI prediction tool (Jia et al., 2017). Virulence factors were searched against the databases VFDB (Chen et al., 2016a) and VirulenceFinder (Joensen et al., 2014), and nucleotide sequences of previously described candidate virulence genes of *Staphylococcus epidermidis* and *S. haemolyticus* (Gill et al., 2005; Takeuchi et al., 2005). To calculate the ANI value, the OrthoANI algorithm implemented on the EzBioCloud server was used (Lee et al., 2016). The dDDH values were calculated using the web-based genome-to-genome distance calculator (GGDC) version 2.1 (Meier-Kolthoff et al., 2013).

2.9. Sequence accession numbers

The whole-genome shotgun projects of strains CCM 8418^T, CCM 8421^T, CCM 8494^T, P5404, and CCM 8529^T have been deposited at GenBank under the accession numbers SRJE00000000, SRJF00000000, SRLF00000000, SRLS00000000, and SRPJ00000000 respectively. Partial *rpoB* gene sequences of strains P4324, P6625, P6635 and P6644 have been deposited at GenBank under the accession numbers MK649779, MK649780, MK649781 and MK649782, respectively.

2.10. Bacteriophage induction and characterization

Prophages were induced from the genome-sequenced strains with mitomycin C as described previously (Pulverer et al., 1974). Phage φSPJ1-int3 (Vb_SpeS_5404) from *S. petrasii* subsp. *jettensis* strain P5404 was propagated on *S. petrasii* subsp. *jettensis* P5402 and further characterized. The phage lysate was purified by zonal centrifugation in a CsCl gradient as described previously (Maslanova et al., 2013). Proteomic analysis of the purified phage was performed by liquid chromatography - mass spectrometry (LC–MS) using an RSLCnano system (Thermo Fisher Scientific) on-line connected to an Impact II Ultra-High Resolution Qq-Time-of-Flight mass spectrometer (Bruker) as described previously (Zeman et al., 2017).

2.11. Electron and cryo-electron microscopy

Negative-stained samples were prepared by staining in 2% uranyl acetate on copper grids coated with a 12-nm continuous carbon layer. Cryo samples were prepared by vitrification of the bacteriophage solution (at a concentration of 10^{10} PFU ml^{-1}) on Quantifoil grids by plunge freezing in liquid ethane using a Thermofisher Scientific Vitrobot Mark IV. The samples were observed with a Thermofisher Scientific Tecnai F20 electron microscope operated at 200 kV at a magnification of 29,000×.

2.12. PCR detection of cas1, cas2 and cas9 genes

Conventional singleplex PCR were carried out in 25 µl reaction mixtures (10 mM Tris-HCl, 50 mM KCl, 1.5 mM $MgCl_2$, 200 µM dNTPs), including 0.2 µM each of primers and 1.5 unit of Taq DNA polymerase (New England Biolabs), and of 50 ng of purified DNA. Primers cas1F (ACAGTTGAAGTGGGAYGAAG) and cas1R (ACCATCAATTTCAACWCGMGCA), cas2F (ATGTTTGATYTRCCTGTAGAAAC) and cas2R (AATGCTCTAACATGYCCTTC) or cas9F (AGAGGYGCGCGTAGATTAAA) and cas9R (AAWGGACTTCCTTCGCCAGG) gave rise to 502 bp, 194 bp or 515 bp products, respectively. Cycling conditions were 5 min denaturation at 96 °C, followed by 25 cycles at 94 °C for 30 s, 55 °C for 30 s and 72 °C for 30 s.

3. Results

3.1. Source and identification of Staphylococcus petrasii

The specimens were recovered from human clinical material, mainly inpatients and a limited number of outpatients, predominantly from young children and older patients in which the pathogenesis of infections was similar as for other CoNS species (Table 1). Over the last 20 years, 3% of CoNS in the NRL/St were retrospectively identified as *S. petrasii* (Fig. S1). Since the majority of the strains were originally misidentified in routine clinical microbiology laboratories, we proposed suitable biochemical tests for the differentiation of *S. petrasii* subspecies from biochemically similar *Staphylococcus warneri*, *S. haemolyticus* and *Staphylococcus auricularis* (Fig. 1).

Specifically, the identification of *S. petrasii* strains was enabled by establishing MALDI-TOF MS as a microbial diagnostic tool. Of the 65 analyzed strains, 6 strains were identified with high confidence and log (score) > 2.0, and 37 with low confidence and log(score) 1.7–2.0, both indicating their assignment as Biotyper database entries *Staphylococcus* sp. 10w414721 RLH, *Staphylococcus* sp. 901400083 LBK, *Staphylococcus* sp. 4 PIM and *Staphylococcus* sp. CS 331_1BRB (all these database strains were assigned as *S. petrasii* in the recently released update of the MBT 8468 MSP Library, version 9.0.0.0). The remaining 22 strains yielded log(score) < 1.7, indicating no significant similarity to any of the database entries. Simply extending the Biotyper database with *S. petrasii* subsp. *petrasii* CCM 8418^T mass spectra resulted in the correct identification of 61 strains with log(score) > 2.0, while only four strains (among them three *S. petrasii* subsp. *pragensis*) were identified with log(score) 1.7–2.0. The MALDI-TOF MS-based cluster analysis (Fig. S2) revealed distinct clusters of *S. petrasii* subsp. *croceilyticus* and *S. petrasii* subsp. *pragensis* strains, while the remaining two subspecies were unresolved. For subspecies identification, further extension of the Biotyper database with *S. petrasii* subsp. *croceilyticus* CCM 8421^T and *S. petrasii* subsp. *pragensis* P6089 resulted in the correct assignment of all strains to the corresponding subspecies. Type strain *S. petrasii* subsp. *pragensis* CCM 8529^T was not found to be a suitable database entry. However, due to the absence of mass spectral features distinctive for *S. petrasii* subsp. *petrasii* and *S. petrasii* subsp. *jettensis*, no database extension that resulted in the correct identification of these two subspecies was designable.

Fingerprinting-based techniques $(GTG)_5$-REP-PCR and automated ribotyping that were previously shown to be effective for subspecies differentiation in staphylococci (Svec et al., 2010) confirmed strain identification at the subspecies level, except for strains P4324, P5414, P6635, P6625, and P6644 (Figs. S3 and S4). Partial *rpoB* gene sequencing was performed in the unassigned isolates and only strain P6644 was classified as *S. petrasii* subsp. *pragensis* (Fig. S5), while the rest remained unidentified to the subspecies level.

3.2. PFGE typing of Staphylococcus petrasii

S. petrasii isolates exhibited 61 different PFGE patterns of 7–14 *Sma*I restriction endonuclease fragments (Fig. 2), demonstrating a high clonal diversity and simultaneously confirming PFGE to be an efficient typing technique. The isolates were separated into three major clusters corresponding to *S. petrasii* subsp. *pragensis*, *S. petrasii* subsp.

Table 1
Origin of *Staphylococcus petrasii* strains characterized in this study.

Material	Patient age group	Number of strains for *S. petrasii* subspecies[a]					Diagnoses
		SPP	SPJ	unassigned	SPC	SPR	
blood culture	0–10	1	–	–	–	–	low birth weight
	40–59	6	2	–	1	2	cerebral hemorrhage, abdominal pain, fever, secondary malignant neoplasm of lymph nodes, acute respiratory failure, gastritis, epilepsy, pancreatitis, sepsis
	60–100	6	6	–	–	–	hospitalization at ICU, stroke, fever, asthmatic bronchitis, hematuria, pneumonia, sepsis, graphite fibrosis of lung
purulence, wound	0–10	1	1	–	–	–	festering wound, low birth weight
	11–39	–	–	–	–	1	finger lesion
	40–59	1	–	–	–	3	multiple head trauma, appendicitis, head abscess
	60–100	1	1	–	–	1	festering wound, cellulitis of torso
skin or cathether swab	70–90	2	2	–	–	–	cellulitis of finger, burn
urine	0–10	1	–	–	1	–	urinary tract infection
	40–59	1	–	–	–	–	acute cystitis
	60–100	–	1	–	–	3	malignant neoplasm of breast, malignant neoplasm of kidney, hyperplasia of prostate
vaginal swab	20–40	2	–	–	–	1	high-risk pregnancy, acute inflammation of vagina
ejaculate	50–60	–	–	–	–	1	chronic prostatitis
ear swab	0–10	2	–	1	3	–	neonatal bacterial sepsis, otitis externa
	20–40	–	–	–	1	–	otitis externa
	60–100	–	1	–	–	–	otitis externa
eye swab	50–60	–	–	1	–	–	–
biopsy	50–60	–	1	1	–	–	–
nose swab	20–40	1	–	–	–	–	carrier
hospital environment	–	1	2	–	–	–	–
unknown human origin	–	–	–	1	–	–	–

[a] SPP, *S. petrasii* subsp. *petrasii*; SPC, *S. petrasii* subsp. *croceilyticus*; SPJ, *S. petrasii* subsp. *jettensis*; SPR, *S. petrasii* subsp. *pragensis*.

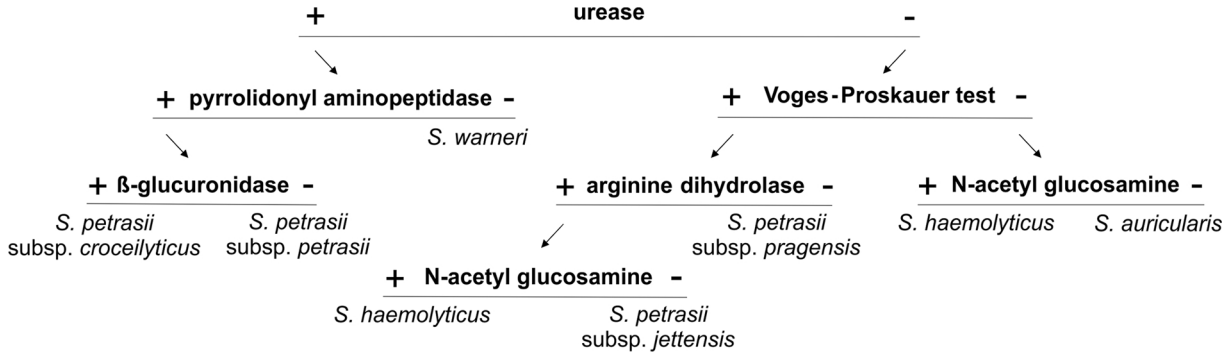

Fig. 1. Biochemical differentiation between *Staphylococcus petrasii* subspecies and phylogenetically related *Staphylococcus haemolyticus* and phenotypically similar *Staphylococcus auricularis* and *Staphylococcus warneri*, performed using commercially available kits. *S. petrasii* strains give a positive reaction in pyrrolidonyl aminopeptidase and Voges-Proskauer tests and do not produce acid from *N*-acetyl glucosamine. The four *S. petrasii* subspecies are easily differentiated from each other by urease, β-glucuronidase and arginine dihydrolase activity tests.

croceilyticus and a cluster of closely related subspecies *S. petrasii* subsp. *petrasii* and *S. petrasii* subsp. *jettensis* at a similarity level of 45%. *S. petrasii* subsp. *jettensis* formed a distinct clade separating at a similarity level of 65% (Fig. 2). Four pairs of strains isolated in the same hospital showed indistinguishable PFGE patterns (Fig. 2), but three pairs differed in their plasmid and antibiotic resistance profiles, indicating that they were not identical clones.

3.3. Antimicrobial susceptibility

Twenty-three percent of the strains were multi-drug resistant, exhibiting resistance to three or more key therapeutic antibiotics, mostly in *S. petrasii* subsp. *jettensis* isolates (Fig. 2). The most prevalent was resistance to benzylpenicillin (63%), erythromycin (28%), clindamycin (22%) and tetracycline (15%). Twenty-eight percent of *S. petrasii* strains did not exhibit resistance to any of the tested antibiotics. Nine *S. petrasii* subsp. *jettensis* strains were resistant to cefoxitin and m*ecA*-positive. The m*ecA* gene was detected only in subspecies *S. petrasii* subsp. *jettensis*, while *mecB* and *mecC* genes were not detected in any of the tested strains. Of the 9 methicillin resistant strains, strain P6318 was resistant to anti-MRSA 5th generation cephalosporins when using ceftaroline disks; additional three strains exhibited intermediate susceptibility. Plasmid profiling showed variable plasmid content in all strains (Fig. 2), represented by one to four plasmids classified into 4 classes according to Novick (Novick, 1990).

3.4. Genome characteristics and comparative genomics

The whole genome sequences of type strains *S. petrasii* subsp. *petrasii* CCM 8418^T, *S. petrasii* subsp. *croceilyticus* CCM 8421^T, *S. petrasii* subsp. *jettensis* CCM 8494^T, and *S. petrasii* subsp. *pragensis* CCM 8529^T and one additional methicillin-resistant *S. petrasii* subsp. *jettensis* P5404 isolate from a fatal case of bronchopneumonia were annotated and characterized (Table 2). The comparison of *S. petrasii* with closely related *S. haemolyticus* showed that *S. petrasii* genomes share 78% orthologous protein clusters, as illustrated by Venn diagram (Fig. 3). The accessory genome of *S. petrasii* subsp. *jettensis* strains is larger than in the other subspecies (Table 2). Distinctive operons encoding saccharide intake transporters and various efflux systems were identified in the *oriC* environ of *S. petrasii* subspecies. The strain *S. petrasii* subsp. *petrasii* CCM

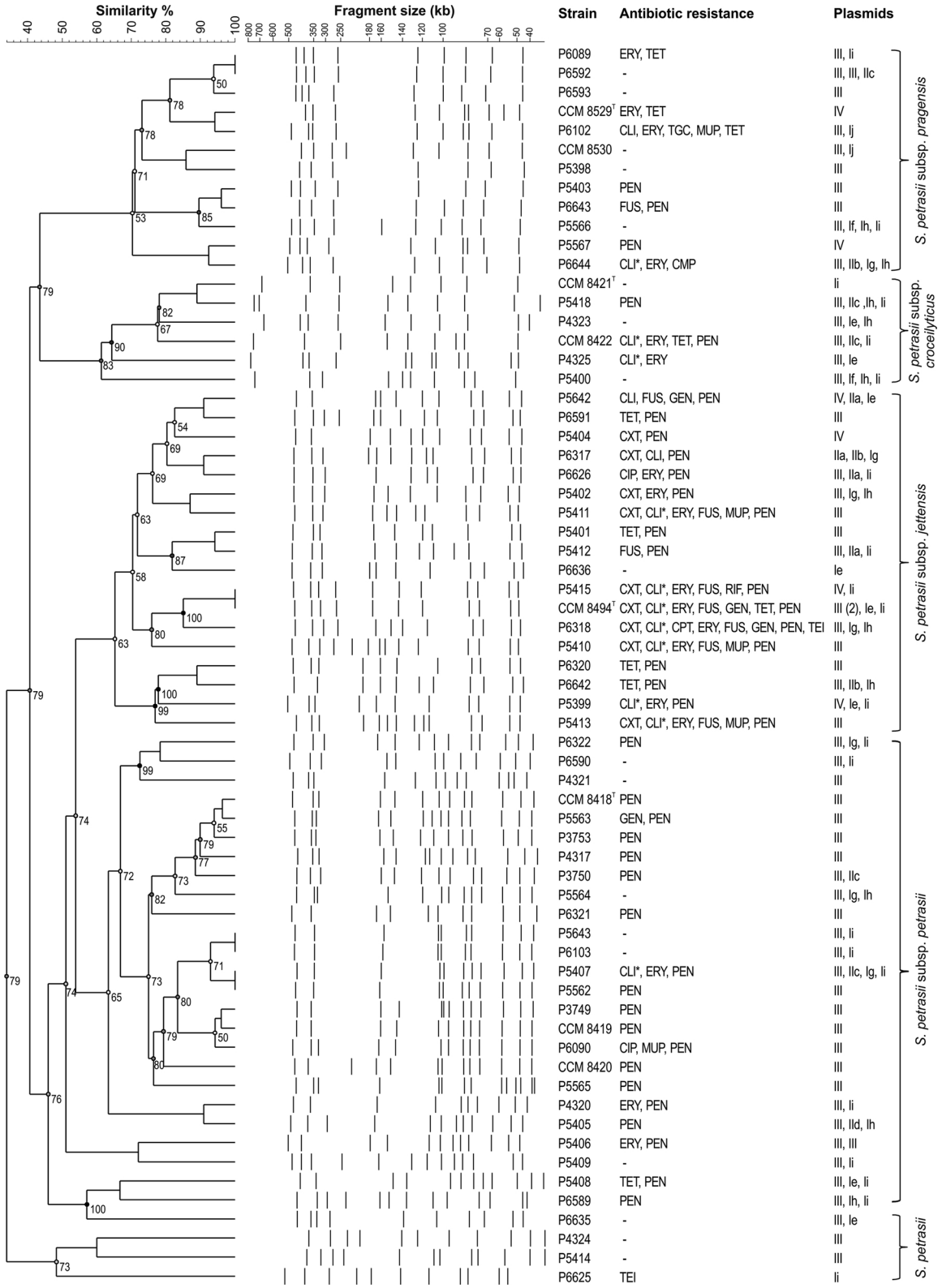

Fig. 2. Dendrogram representing similarity of PFGE patterns of *Sma*I-digested genomic DNA of 65 *Staphylococcus petrasii* strains constructed by UPGMA cluster analysis with Dice similarity coefficients. Antibiotic resistance and plasmid profiles identified in these strains are shown. Plasmids were classified into categories based on their size (I: 1–4.9 kb, II: 5–8 kb, III: 15–30 kb and IV: > 30 kb) and to subgroups designated by lower-case letters based on the different patterns resolved by agarose gel electrophoresis. Antibiotics: CIP - ciprofloxacin, CLI - clindamycin, CLI* - possible inducible resistance for clindamycin, CMP - chloramphenicol, CPT - ceftaroline, CXT - cefoxitin, ERY - erythromycin, FUS - fusidic acid, GEN - gentamicin, MUP - mupirocin, PEN - benzylpenicillin, RIF - rifampicin, TEI - teicoplanin, TET - tetracycline, and TGC - tigecycline.

Table 2
Summary of whole genome sequence characteristics of analyzed *Staphylococcus petrasii* strains.

Genome	S. *petrasii* subsp. *petrasii* CCM 8418^T	S. *petrasii* subsp. *croceilyticus* CCM 8421^T	S. *petrasii* subsp. *jettensis* CCM 8494^T	S. *petrasii* subsp. *jettensis* P5404	S. *petrasii* subsp. *pragensis* CCM 8529^T
WGS Project no.	SRJE00000000	SRJF00000000	SRLF00000000	SRLS00000000	SRPJ00000000
Size (bp)	2478122	2371527	2709607	2620440	2447231
Contigs > 500 bp	12	43	54	55	18
N50	879073	148481	140928	145653	396835
GC content (mol%)	33.32	33.31	33.24	33.31	33.06
GC content of core genome (mol%)	33.44	33.34	33.46	33.39	33.22
Total genes	2462	2322	2670	2559	2438
Protein coding sequences	2381	2240	2588	2482	2366
Genes with clusters of orthologous gropus	2246	2132	2362	2362	2197
Genes on mobile genetic elements and the genome percentage they represent	165 (6%)	37 (2%)	360 (12%)	270 (9%)	200 (7%)
Prophages	φSPP-int1 (43.1 kb)	–	φSPJ-int3 (45.2 kb), φSPβ-like (125 kb)	φSPJ-int2 (42.9 kb), φSPJ-int3 (45.1 kb)	φSPR-int2 (40.9 kb)
SCC elements	$SCC_{CCM8418}$ (27 kb)	SpCI-$SCC_{CCM8421}$ (35.3 kb)	SpCI-SCC*mec*$_{CCM8494}$ (68.9 kb)	SpCI-SCC*mec*$_{P5404}$ (102.5 kb)	ψ$SCC_{CCM8529}$ (43 kb)
Plasmids	pVVSP1 (class III)	pVVSC1 (class I)	pVVSJ1 (class I), pVVSJ2 (class I), pVVSJ3 (clas III), pVVSJ4 (class III)	pVVSJ5 (class IV)	pVVSR1 (class IV)
Phage-inducible chromosomal islands	SpCI-$1_{CCM8418}$ (12.4 kb), SpCI-$2_{CCM8418}$ (16.3 kb)	–	SpCI-$1_{CCM8494}$ (16.3 kb)	–	SpCI-$1_{CCM8529}$ (15.6 kb), SpCI-$2_{CCM8529}$ (13.6 kb), SpCI-$3_{CCM8529}$ (14.2 kb)
Other chromosomal island	–	–	–	–	SpCI-$4_{CCM8529}$ (12 kb)
Transposones	Tn*554*-like	–	Tn*554*-like	Tn*554*-like	Tn*5406*-like
IS elements	–	IS*1182* (5 copies), IS*3* (3 copies), IS*30* family (4 copies)	IS*6* (4 copies), IS*1186* family (7 copies)	IS*6* (9 copies), IS*1186* family (5 copies)	IS*30* family (6 copies)
RM systems	type I (incomplete - *hsdSR*), type IV (*mcrBC*)	type I (*hsdMSR*), type IV (*mcrBC*)	type I (*hsdMSR*), type IV (*mcrBC*)	type I (*hsdMSR*), type IV (*mcrBC*)	type IV (*mcrBC*)
CRISPR	–	–	type II-C	type II-C	type II-C

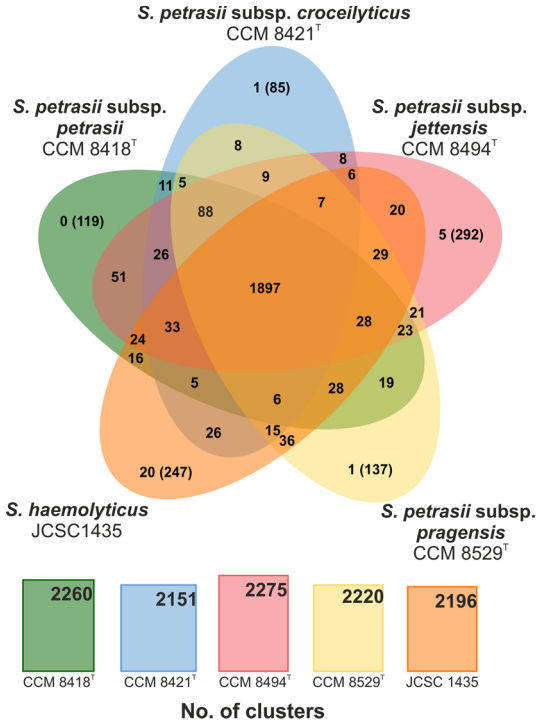

Fig. 3. Venn diagram representing orthologous protein clusters shared between genomes of type strains of *Staphylococcus petrasii* subspecies and *Staphylococcus haemolyticus* JCSC1435 (Takeuchi et al., 2005). The number of singletons for each genome is shown in brackets.

8418^T carries putative phosphotransferase transporter systems (PTSs) for mannitol and mannose in the *oriC* environ. In strain *S. petrasii* subsp. *croceilyticus* CCM 8421^T, pathways for saccharide conversion to pyruvate were predicted, including major facilitator superfamily hexose transporter or glycoside-pentoside-hexuronide transporter. Strains *S. petrasii* subsp. *jettensis* CCM 8494^T and P5404 differ from the other subspecies in the presence of an operon with predicted glutathione transporter and gamma-glutamyl transferase gene involved in cysteine biosynthesis.

Comparative genome analyses revealed the presence of many MGE as the major source of genome variability (Fig. 4). Plasmids, genomic islands including SCC, transposones, and a φSPβ-like prophage provided the strains of *S. petrasii* with resistance genes and genes promoting survival in the environment (Table 3). Additionally, SCC-like elements and the φSPβ-like prophage carry genes enhancing the virulence of the strains (Table 4). Other virulence factors such as global regulators, exoenzymes and surface proteins promoting biofilm formation and host immune system evasion are mainly found in the core genome and are similar to the virulence genes of *S. haemolyticus*.

SCC elements are present in all analysed genomes, inserted in the *rlmH* (*orfX*) gene (Table 2, Fig. 4). *S. petrasii* subsp. *petrasii* CCM 8418^T and *S. petrasii* subsp. *pragensis* CCM 8529^T have a single cassette (Fig. 5). The $SCC_{CCM8418}$ element harbours the *ccrA5B3* gene complex, whereas in the $\psi SCC_{CCM8529}$ element the *ccr* genes are absent. *S. petrasii* subsp. *croceilyticus* CCM 8421^T and both *S. petrasii* subsp. *jettensis* strains CCM 8494^T and P5404 carry composite chromosomal islands (CIs) (Fig. 5). SpCI-$SCC_{CCM8421}$ has a mosaic structure composed of 17.6-kb $SCC1_{CCM8421}$ and 17.7-kb $SCC2_{CCM8421}$, which harbour the *ccr* gene complexes *ccrA4B4* and *ccrC*, respectively. The largest CIs are present in *S. petrasii* subsp. *jettensis* and both CIs confer methicillin resistance by carrying *mecA* gene complexes. SpCI-$SCCmec_{CCM8494}$ is composed of a

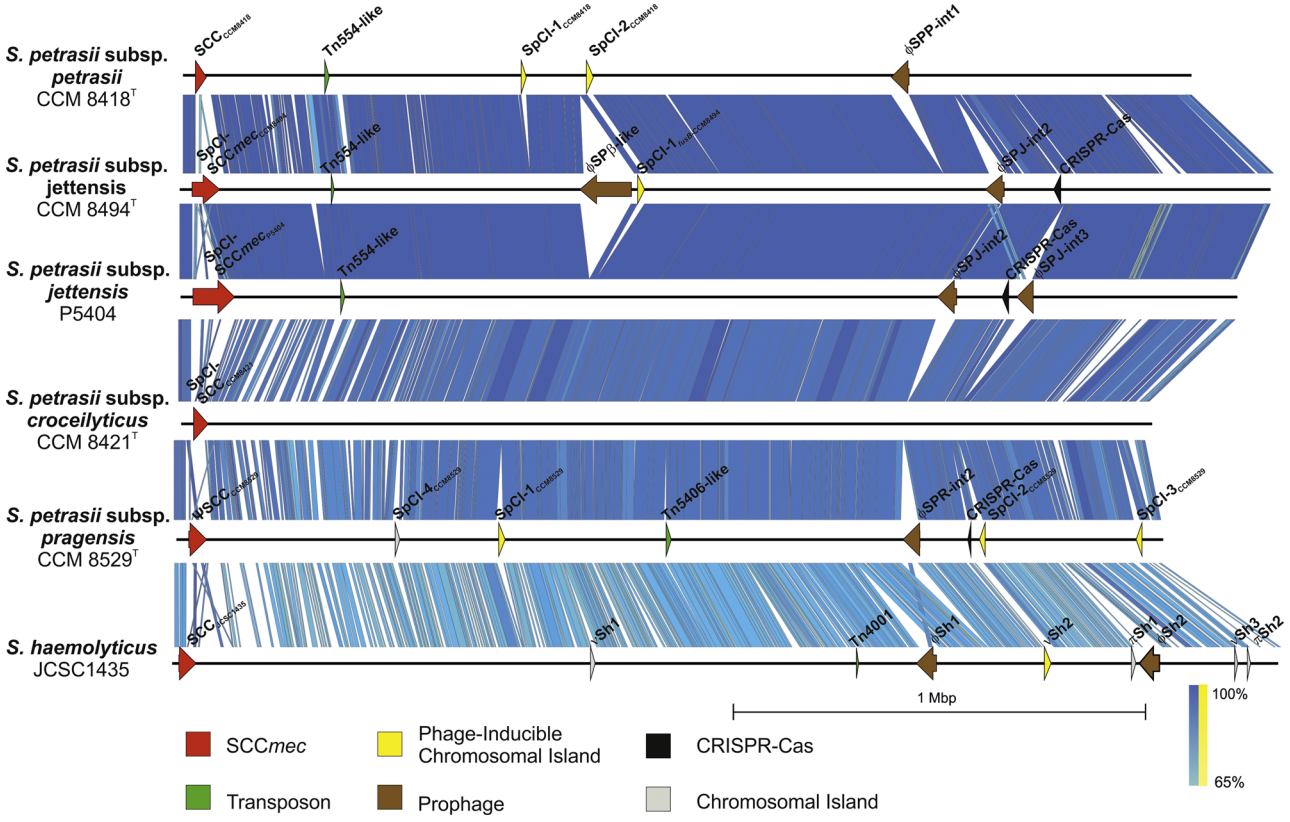

Fig. 4. Whole-genome comparison of *Staphylococcus petrasii* subsp. *petrasii* CCM 8418^T (GenBank accession number SRJE00000000), *S. petrasii* subsp. *croceilyticus* CCM 8421^T (SRJF00000000), *S. petrasii* subsp. *jettensis* CCM 8494^T (SRLF00000000) and P5404 (SRLS00000000), *S. petrasii* subsp. *pragensis* CCM 8529^T (SRPJ00000000) and *Staphylococcus haemolyticus* JCSC1435 (AP006716) with a focus on variable genetic elements. Conserved regions with more than 65% homology are indicated in blue, inversions in yellow as determined by blastn.

Table 3
Antibiotic resistance genes and response to environmental stimuli genes, their functions and locations on mobile genetic elements.

Mechanism	Gene(s)	Function	Strain and location on mobile genetic elements				
			CCM 8418^T	CCM 8421^T	CCM 8494^T	P5404	CCM 8529^T
Antibiotic resistance	AAC(6')-Ie-APH(2")-Ia	aminoglycoside antibiotic resistance	–	–	φSPβ-like	–	–
	APH(3')-IIIa	aminoglycoside antibiotic resistance	–	–	φSPβ-like	–	–
	ANT(6)-Ia	aminoglycoside antibiotic resistance	–	–	φSPβ-like	–	–
	ANT(4')-Ib	aminoglycoside antibiotic resistance	–	–	–	pVVSJ4	–
	blaZ	penam antibiotic resistance	Tn*554*-like	–	Tn*554*-like	Tn*554*-like, pVVSJ5	–
	mecA	penam, monobactam, carbapenem, cephamycin, cephalosporin antibiotic resistance	–	–	SCC*mec*$_{CCM8494}$	SCC*mec*$_{P5404}$	–
	ermC	streptogramin antibiotic, macrolide antibiotic, lincosamide antibiotic resistance	–	–	pVVSJ2	–	–
	fusB	fusidic acid resistance	–	–	SpCI-1$_{fusB\text{-}CCM8494}$	–	–
	msrA	streptogramin antibiotic, macrolide antibiotic resistance	–	–	–	pVVSJ5	pVVSR1
	mphC	macrolide antibiotic resistance	–	–	–	pVVSJ5	pVVSR1
	tet(K)	tetracycline antibiotic resistance	–	–	–	–	pVVSR1
	mupA	mupirocin resistance	–	–	–	pVVSJ5	–
	vgaA	streptogramin antibiotic resistance	–	–	–	–	Tn*5406*-like
	qacABR	multidrug efflux system	–	–	–	–	pVVSR1
	qacC	multidrug efflux system	–	pVVSC1	pVVSJ1	pVVSJ5	–
Response to environmental stimuli	*arsCBAD*	arsenic resistance operon	SCC$_{CCM8418}$	–	–	–	ψSCC$_{CCM8529}$
	cadD	cadmium transporter	pVVSP1	–	pVVSJ4	pVVSJ5	pVVSR1
	cadX	transcriptional regulator, cadmium resistance	pVVSP1	–	pVVSJ4	pVVSJ5	pVVSR1
	merR	transcriptional regulator, mercuric ion resistance	pVVSP1	–	pVVSJ4	–	–
	mntH	manganese transporter	–	–	pVVSJ3	pVVSJ5	–
	sulP	sulphate transporter family protein	–	–	pVVSJ3	–	pVVSR1
	USP	universal stress protein	–	–	pVVSJ3	–	pVVSR1
	LTTRs	LysR-type transcriptional regulators	–	–	–	–	pVVSR1
	sunT	ABC-type bacteriocin transporter	pVVSP1	–	–	pVVSJ5	–
	trkG	potassium pump component	–	–	–	–	SpCI-1$_{CCM8529}$
	RuMP pathway	formaldehyde detoxification	–	–	pVVSJ3	pVVSJ5	pVVSR1

Table 4
Candidate virulence factors found in sequenced *Staphylococcus petrasii* strains representing homologs with known and previously predicted virulence factors.

Function and role	Gene(s)	Product	Strain and location				
			CCM 8418^T	CCM 8421^T	CCM 8494^T	P5404	CCM 8529^T
Global regulation system	*agrA-D*	response regulator	ch.	ch.	ch.	ch.	ch.
		accessory gene regulator B	ch.	ch.	ch.	ch.	ch.
		receptor histidine kinase	ch.	ch.	ch.	ch.	ch.
		agrD protein	ch.	ch.	ch.	ch.	ch.
	sarARVZ	staphylococcal acessory regulators	ch.	ch.	ch.	ch.	ch.
	arlRS	two component regulatory system	ch.	ch.	ch.	ch.	ch.
	rot	repressor of toxins	ch.	ch.	ch.	ch.	ch.
	sigB	alternative sigma factor	ch.	ch.	ch.	ch.	ch.
Surface adhesins and biofilm formation	*fbe*	fibrinogen binding protein	ch.	ch.	ch.	ch.	ch.
	ebpS	elastin binding protein	ch.	ch.	ch.	ch.	ch.
	atlE	bifunctional alutolysin	ch.	ch.	ch.	ch.	ch.
	sasADH	cell wall surface anchors	ch.	ch.	ch.	ch.	ch.
	mntABC	transporter	ch.	ch.	ch.	ch.	ch.
MSCRAMMs	*sdrC*	serine-asparate repeat proteins	ch.	ch.	ch.	ch.	ch.
	sdrH	serine-asparate repeat proteins	ch.	ch.	ch.	ch.	ch.
Exoenzymes	*hlyIII*	hemolysin III	ch.	ch.	ch.	ch.	ch.
	clpP	clp protease, proteolytic subunit	ch.	ch.	ch.	ch.	ch.
	clpBCX	clp protease, ATP binding subunits	ch.	ch.	ch.	ch.	ch.
	htrA	htrA like protease, putative	ch.	ch.	ch.	ch.	ch.
	splE/splF	serine protease	ch.	ch.	ch.	ch.	ch.
	rseP	zinc metalloprotease	ch.	ch.	ch.	ch.	ch.
	lysM	putative peptidoglycan binding domain	ch.	ch.	ch.	ch.	ch.
	nanA	sialic acid lyase	ch.	ch.	ch.	ch.	ch.
	pldB	lysophospholipase	ch.	ch.	ch.	ch.	ch.
	lipA	lipase/esterase	ch.	ch.	ch.	ch.	ch.
	aes	acetyl sterase	ch.	ch.	ch.	ch.	ch.
	sbcCD	exonucleases	ch.	ch.	ch.	ch.	ch.
Capsule formation	*capA-P*	capsule biosynthesis proteins	ch.	ch.	ch.	ch.	ch.
	oatA	o-acetyltransferase	ch.	ch.	ch.	ch.	ch.
	cpsE	glycosyltransferase	ch.	ch.	ch.	ch.	ch.
Immunomodulation	*psm*β1β2	phenol-soluble modulins β1 and β2	ch.	ch.	ch.	ch.	ch.
	*psm*γ/*hld*	delta toxin	ch.	ch.	ch.	ch.	ch.
	isaAB	immunodominant antigens	ch.	ch.	ch.	ch.	ch.
	sceD	immunodominant antigen	ch.	ch.	ch.	ch.	ch.
	pls	plasmin-sensitive surface protein	–	–	SpCI-SCC*mec*$_{CCM8494}$	SpCI-SCC*mec*$_{P5404}$	ψSC$_{CCCM8529}$
Other virulence and putative virulence genes	*sasX*	surface-anchored protein	–	–	φSPβ-like	–	–
	abpE	flavin transferase	–	SpCI-SCC$_{CCM8421}$	–	–	ψSCC$_{CCM8529}$
	flaR	flavin reductase	–	SpCI-SCC$_{CCM8421}$	–	–	ψSCC$_{CCM8529}$
	norB	nitric oxide reductase	–	SpCI-SCC$_{CCM8421}$	–	–	ψSCC$_{CCM8529}$
	speG	spermidine N-acetyltransferase	SCC$_{CCM8418}$	SpCI-SCC$_{CCM8421}$	–	–	ψSCC$_{CCM8529}$
	yeiMCN	pseudouridine utilization pathway	–	SpCI-SCC$_{CCM8421}$	SpCI-SCC*mec*$_{CCM8494}$	SpCI-SCC*mec*$_{P5404}$	–
	srlBEAMRD	sorbitol utilization operon	–	–	–	SpCI-SCC*mec*$_{P5404}$	–
	LTTRs	LysR-type transcriptional regulators	–	–	–	–	pVVSR1
	cstABR	hydrogen sulphide detoxification cluster	–	–	SpCI-SCC*mec*$_{CCM8494}$	SpCI-SCC*mec*$_{P5404}$	–

Legend: ch., chromosome.

29.9-kb SCC*mec*$_{CCM8494}$ type VIII (4A) and SpCI-SCC*mec*$_{P5404}$ harbours a 38.3-kb SCC*mec*$_{P5404}$ type V (5C2&5). Also, both CIs have almost the same 39.0-kb SCC element designated SCC$_{P5404}$ and/or SCC$_{CCM8494}$ with recombinases *ccrA1B3*. SpCI-SCC*mec*$_{P5404}$ has an additional 25.2-kb SCC$_{sorbitol-P5404}$ element with *ccrA1B1* genes and a sorbitol phosphotransferase operon. SCCs contain putative virulence genes for plasmin-sensitive surface proteins (*pls*) and spermidine N-acetyltransferase (*speG*), a cluster of *apbE*, flavin reductase, and *norB* and a cluster of *yeiMNC* for the uptake and catabolism of pseudouridine (Table 4, Fig. 5).

All sequenced genomes except that of *S. petrasii* subsp. *croceilyticus* contain prophages with a typical siphoviral modular structure (Fig. S6). Three phage integrase types were identified, determining prophage insertion into tRNA-Arg-TCT (φSPP-int1), tRNA-Ser-GCT (φSPR-int2 and φSPJ-int2) or near the CRISPR locus (φSPJ-int3) (Fig. 4). Double lysogenic host strain *S. petrasii* subsp. *jettensis* P5404 produced viable

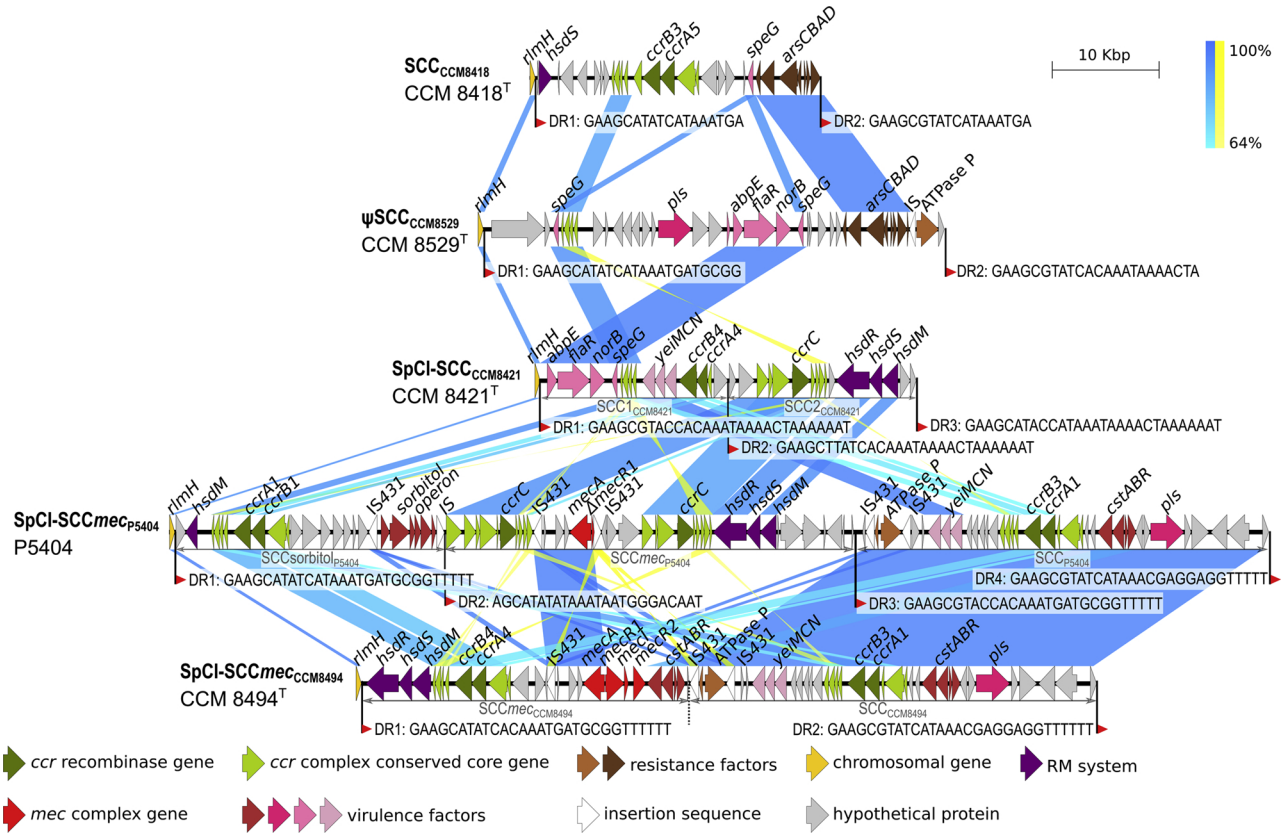

Fig. 5. Comparative analysis of staphylococcal cassette chromosome (SCC) inserted in *rlmH* gene harboured by *Staphylococcus petrasii* subspecies. Predicted coding sequences (ORFs) are depicted in the direction of transcription as arrows. Core genes of the SCC elements, genes for virulence and resistance factors, insertion sequences and genes for RM system are annotated. Sequences of direct repeats are shown below the ORF maps. Conserved regions with more than 64% homology are indicated in blue as determined by blastn.

Siphoviridae phage particles (Fig. 6) and LC–MS analysis of the phage structural proteins found a match with the prophage φSPJ-int3 (Vb_SpeS_5404). In the *S. petrasii* subsp. *jettensis* CCM 8494^T genome, a 125-kb-long φSPβ-like converting prophage integrated into a gene encoding a YeeE/YedE family protein was found (Fig. 4). The prophage carries aminoglycoside resistance genes and a *sasX* gene homologue considered to be a virulence factor.

Six types of phage-inducible chromosomal islands (PICIs) with lengths of 12–16 kb contributing to host adaptation and virulence were identified (Table 2, Fig. 4). SpCI-1$_{fusB\text{-}CCM8494}$ carries the fusidic acid family resistance determinant *fusB*. This island has the common *att* insertion site AATGACATAA with *S. petrasii* subsp. *petrasii* SpCI-2$_{CCM8418}$ in the *groEL* gene encoding a heat shock protein. Insertion site (*att*) TTGAATACGT in the lactose operon is shared by *S. petrasii* subsp. *petrasii* SpCI-1$_{CCM8418}$ and *S. petrasii* subsp. *pragensis* SpCI-1$_{CCM8529}$, which harbour a *trkG* gene homologue encoding a putative potassium transporter component. *S. petrasii* subsp. *pragensis* SpCI-2$_{CCM8529}$ and SpCI-3$_{CCM8529}$ are integrated into the tmRNA gene *ssrA* and glutamine amidotransferase protein gene *guaA*, respectively. The novel chromosomal island SpCI-4$_{CCM8529}$ with putative genes for methylation with a potential role in DNA protection and repair was found in the strain CCM 8529^T (Fig. 4, Table 2).

Extrachromosomal plasmids were identified in all the sequenced genomes (Table 2), encoding antimicrobial resistance genes enabling survival in adverse environments (Table 3). Small *S. petrasii* plasmids pVVSJ1, pVVSJ2, and pVVSC1 encode multidrug efflux system *qacC* or erythromycin resistance *ermC* genes (Table 3). Plasmids pVVSP1, pVVSJ3, and pVVSR1 carried a *traA* relaxase gene homologue that participates in conjugation. The plasmids pVVSJ3, pVVSJ5, and pVVSR1 carry the formaldehyde detoxification operon with the ribulose monophosphate pathway (RuMP) (Fig. S7). Plasmid pVVSJ3 encode membrane protein TcaA, whose inactivation may lead to teicoplanin resistance (McCallum et al., 2007).

Type II-C CRISPR-Cas systems were identified in the genomes of the strains *S. petrasii* subsp. *jettensis* CCM 8494^T and P5404 and *S. petrasii* subsp. *pragensis* CCM 8529^T (Table 2, Fig. 4). Genes *cas1, cas2*, and *cas9* identified in all *S. petrasii* subsp. *pragensis* and *S. petrasii* subsp. *jettensis* strains by PCR screening indicate the prevalence of the CRISPR-Cas system in these two subspecies. The CRISPR locus of *S. petrasii* subsp. *jettensis* is 497 bp long, with 7 spacers separated by eight 36-bp-long repeats GTTTCACTTATACCTAAAATTACAGAGTACTAAAAC that were identical in both sequenced strains. The CRISPR locus of *S. petrasii* subsp. *pragensis* CCM 8529^T is 1684 bp long, with 25 spacers separated by 26 36-bp-long repeats GTCTCACTTATACCTAAAATTACAGAGTACT AAAAC. The *hsdMSR* and *mcrBC* restriction-modification (RM) systems present in all strains (Table 2) are another protection mechanism against DNA uptake. The *S. petrasii* subspecies share probably new type IV RM system based on the low homology with known *mcrBC* genes.

4. Discussion

Since the pathogenic significance and nosocomial spread of CoNS is increasing (Yu et al., 2017), it is particularly important to analyse the virulence potential and epidemiology of blood culture isolates and infections associated with the use of medical devices. One third of *S. petrasii* isolates originated from such specimens, dominated by *S. petrasii* subsp. *petrasii* and *S. petrasii* subsp. *jettensis*, indicating their importance in human disease. The precise identification of *S. petrasii* subspecies can be a prediction of clinical significance, especially due to the multiple drug resistance and methicillin resistance of *S. petrasii*

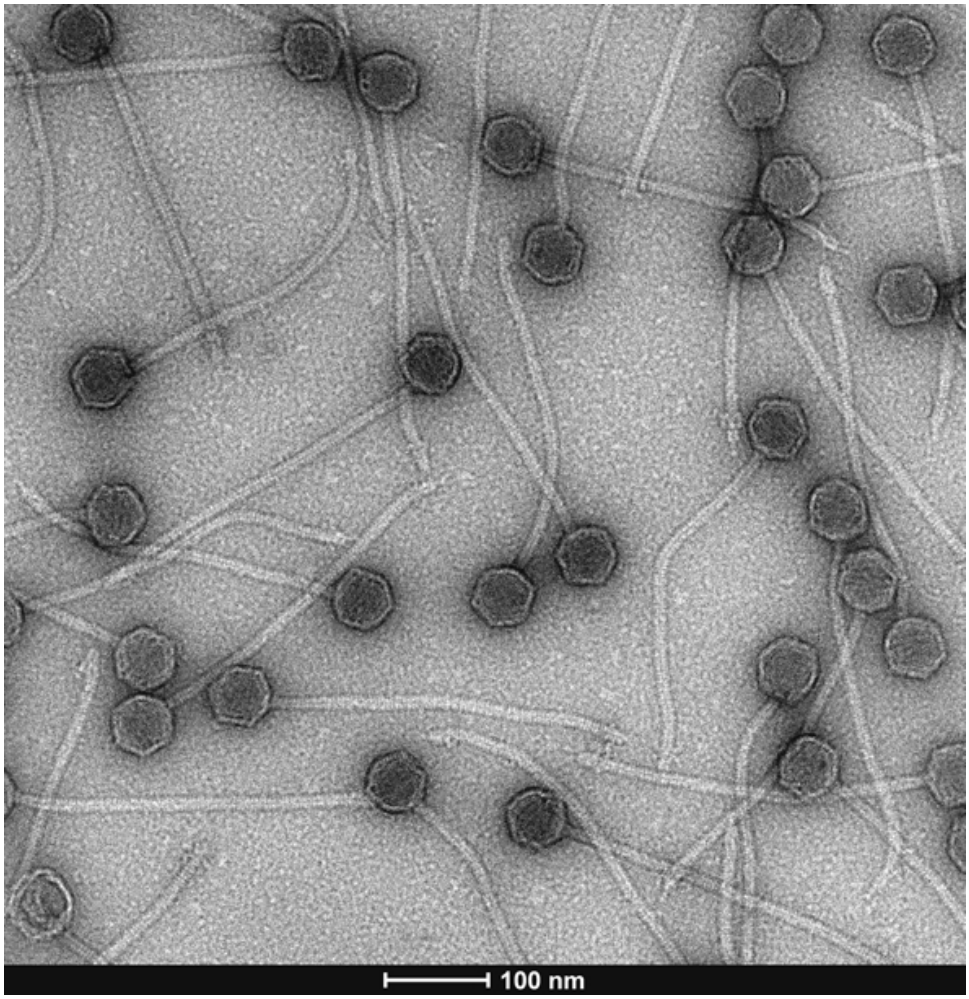

Fig. 6. Transmission electron microscopy image of negatively stained particles of phage φSPJ1-int3 (Vb_SpeS_5404) induced from *Staphylococcus petrasii* subsp. *jettensis* strain P5404 with mitomycin C. The phage particles consist of an icosahedral head (B1 morphology) with diameter 60 nm, flexible, non-contractile 335 nm long and 14 nm wide tail ending with a grape-shaped base plate. The base plate is 40 nm long and 22 nm wide at its upper part.

subsp. *jettensis*. MALDI-TOF MS, PFGE typing, and genome comparison concluded that *S. petrasii* subsp. *petrasii* and *S. petrasii* subsp. *jettensis* are closely related. However, *S. petrasii* subsp. *jettensis* has accumulated more genes in the accessory genome compared to all other subspecies. This could be analogous to the relationship between two *S. hominis* subspecies, where *S. hominis* subsp. *novobiosepticus* exhibits a larger chromosome (Kloos et al., 1998) and significantly higher number of antibiotic resistance genes than *S. hominis* subsp. *hominis* (Fitzgibbon et al., 2001). Unambigous distinguishing between *S. petrasii* subsp. *petrasii* and *S. petrasii* subsp. *jettensis* is possible through biochemical tests, ribotyping and $(GTG)_5$-REP-PCR. On the other hand, all the performed analyses demonstrated clear differentiation of *S. petrasii* subsp. *croceilyticus* and *S. petrasii* subsp. *pragensis*, both from each other and from the other subspecies. Both taxa might be reclassified in the future to different species based on the obtained average nucleotide identity (ANI) values (Table S2).

The comparative genome analysis enables the assessment of the pathogenic potential, mechanisms of host adaptation and survival in the environment, and understanding the evolutionary events associated with horizontal gene transfer (HGT). The *S. petrasii* virulence factors and MGE *att* sites are similar to *S. haemolyticus*, reflecting their evolutionary relatedness. Similar to *S. haemolyticus*, the *S. petrasii* genomes lack the *ica* operon essential for biofilm formation, yet the presence of genes for phenol-soluble modulins promoting biofilm dissemination suggests the existence of an *ica*-independent pathway (Arciola et al., 2015; Panda and Singh, 2018). Genes in the *oriC* environ, which was earlier described as highly variable in staphylococci (Takeuchi et al., 2005), play a crucial role in pathogenesis and adaptation to various host environments. The locus contains various saccharide/pentose uptake systems that enable the utilization of specific substrates. These systems distinguish one staphylococcal species from another, and can be considered to be virulence factors (Siebold et al., 2001; Zuniga et al., 2005). Mannitol-specific PTSs in the *oriC* environ of *S. petrasii* subsp. *petrasii* CCM 8418^T exhibited similarity to that of *S. haemolyticus* and *S. aureus* with 86.5% and 73.6% nucleotide identity, respectively, and this locus is likely horizontally transferred (Takeuchi et al., 2005; Zuniga et al., 2005).

SCC elements located in the *oriC* environ of *S. petrasii* have an extensive mosaic structure with regions homologous to SCC elements from other *Staphylococcus* species supporting the role of HGT in their formation. Despite the fact that nowadays *mecC* is more frequently reported from CoNS (Harrison et al., 2014, 2013; Pantucek et al., 2018) and *mecB* was found in staphylococci (Becker et al., 2018), only *mecA*-carrying SCC*mec* were detected in the *S. petrasii* strains. The $SCC_{CCM8418}$ element has a *ccr* complex similar to *S. haemolyticus* SH32 (Yu et al., 2014) and has a similar heavy-metal-resistance gene structure to *S. aureus* type IX SCC*mec* (Li et al., 2011). The major part of SpCI-$SCC_{CCM8421}$ corresponds to the CI in MRSA isolate M06/0171 (Kinnevey et al., 2013). Significant similarities in gene organization and the presence of a sorbitol-specific PTS system were found between the SpCI-

SCC*mec*$_{P5404}$ and *S. aureus* SCC*mec*$_{WA\text{-}MRSA\text{-}40}$-CI (Wilson et al., 2016). The cluster of SCC-harboured genes *apbE*, *flaR*, *norB*, and *speG* probably promote survival in host cells and confer resistance to host-derived polyamines (Joshi et al., 2011; Morozov et al., 2018; Truong-Bolduc et al., 2011). *Pls* genes can promote the immune system evasion (Werbick et al., 2007) and the genes *yeiMNC* might be beneficial in urinal or ocular infections, as was suggested previously (Sadaka et al., 2014). Most of the *S. petrasii* SCC elements possessed RM systems or their remnants similar to other staphylococci, which could stabilize the SCC elements in the genome (Hanssen and Sollid, 2006; Ito et al., 2004).

The pathogenic potential of the strains is enhanced by the presence of additional MGE in the genomes. The φSPβ-like prophage in *S. petrasii* subsp. *jettensis* CCM 8494^T harbouring the *sasX* gene has almost 99% nucleotide identity with other φSPβ-like prophages, including that of *S. aureus* TW20 (Holden et al., 2010). Li et al. (2012) showed that the *sasX* gene, which is a homologue of *sesI* from *S. epidermidis*, plays a key role in colonization and immune evasion. Compared to *S. aureus* pathogenicity islands, no virulence factors were predicted on *S. petrasii* PICIs that carry many unique ORFs of unknown functions. The only identified resistance gene was *fusB* localized on SpCI-1$_{fusB\text{-}CCM8494}$, exhibiting a similar structure to the SeRI$_{fusB\text{-}704}$ of *S. epidermidis* (Chen et al., 2011). As was found in the *S. haemolyticus* genome (Takeuchi et al., 2005), the presence of IS elements leads to frequent genome rearrangements, that were also observed in strains from the *S. petrasii* complex before its valid taxonomic description (Bartell et al., 2008).

Plasmids that were ubiquitously present in the analyzed set of *S. petrasii* strains carried genes for antibiotic and heavy metal resistance or genes for the response to environmental stimuli. Such an association between heavy metal and antibiotic resistance has been reported earlier, identified mostly in environmental isolates (Baker-Austin et al., 2006) but also in clinical specimens (Zhai et al., 2016). Large plasmids exhibited presence of numerous IS*6* family elements establishing their modular structure. Conserved plasmid segments encoding RuMP and its reverse reaction pathway, which mediate formaldehyde fixation to ribulose-5-phosphate and further metabolization, are proposed to participate in the detoxification of formaldehyde generated by the host metabolism or during heme degradation (Chen et al., 2016b). The same metabolic pathway was observed in modular plasmids of *S. aureus* and other clinically important pathogens (Chen et al., 2016b).

The very high prevalence of CRISPR-Cas systems among *S. petrasii* subsp. *jettensis* and *S. petrasii* subsp. *pragensis* strains is unusual in comparison with CoNS reviewed previously (Rossi et al., 2017). The CRISPR-Cas system might thus protect the host against foreign DNA. The spacers in both subspecies target the sequence of *Siphoviridae* phages of different CoNS (Deghorain et al., 2012; Liu et al., 2018). This could be connected with their occurrence in environments with various bacterial populations in which their bacteriophages participate in HGT. Phages use as their receptors wall teichoic acids (WTA), which composition is crucial for efficient phage mediated HGT (Winstel et al., 2013). When analysing *S. petrasii* WTA-encoding genes, similarities of *tagO*, *mnaA*, cluster *tagAHGBXD-pbp4-tagF*, *tagNV* and *dtlABCD* loci were found to related CoNS. The highest nucleotide similarity 75–85% for *tag* genes and 80–90% for *dtl* genes was found with their homologues from *S. hominis*, *S. lugdunensis* and *S. haemolyticus*, which have the WTA composition Gro-GlcNAc (α) or (α + β) (Endl et al., 1984). The strain CCM 8529^T lacks the *tagN* gene suggesting difference in glycosylation. We hypothesize that WTA composition does not exclude phage mediated HGT.

These results provide an insight into the functional organization of the *S. petrasii* genomes. The presence of many putative virulence factors and antimicrobial resistance genes indicates that this species could be confirmed to be a significant opportunistic pathogen, as occurred with *Staphylococcus lugdunensis* (Argemi et al., 2017). The frequent similarities of *S. petrasii* MGE with other CoNS and *S. aureus* indicate that HGT is important in the spread of the elements or their parts. The reliable *S. petrasii* diagnostics proposed here and its genomic characteristics enable clinical microbiologists to interpret the significance of the species in clinical samples and obtain surveillance data for studying its epidemiology.

Funding

The work was supported by the Czech Science Foundation grant (18-13064S) to R.P. Electron microscopy analyses performed by M.S. were supported by National Sustainability Programme II, project CEITEC 2020 from the Ministry of Education, Youth and Sports of the Czech Republic (LQ1601). P.P. was supported by a project from the Ministry of Health of the Czech Republic – DRO (NIPH, 75010330). V.V., V.K., A.I., and L.F. were supported by the Grant Agency of Masaryk University (MUNI/A/0958/2018). The work was also supported from European Regional Development Fund-Project "CIISB4HEALTH" (No. CZ.02.1.01/0.0/0.0/16_013/0001776). CIISB research infrastructure project LM2015043 funded by the Ministry of Education, Youth and Sports of the Czech Republic is gratefully acknowledged for the financial support of the MS measurements at the Proteomics Core Facility.

Declaration of Competing Interest

All the authors declare no conflicts of interest.

Acknowledgments

The authors would like to thank their colleagues from the participating hospitals for providing the CoNS isolates and patient data.

Appendix A. Supplementary data

Supplementary material related to this article can be found, in the online version, at doi:https://doi.org/10.1016/j.ijmm.2019.151355.

References

Arciola, C.R., Campoccia, D., Ravaioli, S., Montanaro, L., 2015. Polysaccharide intercellular adhesin in biofilm: structural and regulatory aspects. Front. Cell. Infect. Microbiol. 5, 7. https://doi.org/10.3389/fcimb.2015.00007.

Argemi, X., Hansmann, Y., Riegel, P., Prevost, G., 2017. Is *Staphylococcus lugdunensis* significant in clinical samples? J. Clin. Microbiol. 55, 3167–3174. https://doi.org/10.1128/JCM.00846-17.

Aziz, R.K., Bartels, D., Best, A.A., DeJongh, M., Disz, T., Edwards, R.A., Formsma, K., Gerdes, S., Glass, E.M., Kubal, M., Meyer, F., Olsen, G.J., Olson, R., Osterman, A.L., Overbeek, R.A., McNeil, L.K., Paarmann, D., Paczian, T., Parrello, B., Pusch, G.D., Reich, C., Stevens, R., Vassieva, O., Vonstein, V., Wilke, A., Zagnitko, O., 2008. The RAST server: rapid annotations using subsystems technology. BMC Genomics 9, 75. https://doi.org/10.1186/1471-2164-9-75.

Baker-Austin, C., Wright, M.S., Stepanauskas, R., McArthur, J.V., 2006. Co-selection of antibiotic and metal resistance. Trends Microbiol. 14, 176–182. https://doi.org/10.1016/j.tim.2006.02.006.

Barros, E.M., Ceotto, H., Bastos, M.C.F., dos Santos, K.R.N., Giambiagi-deMarval, M., 2012. *Staphylococcus haemolyticus* as an important hospital pathogen and carrier of methicillin resistance genes. J. Clin. Microbiol. 50, 166–168. https://doi.org/10.1128/Jcm.05563-11.

Bartell, J.G., Dajcs, J.J., Ward, D.O., Zentz, E.B., Briska, A.M., Stroman, D.S., 2008. Characterization of staphylococcal isolates by traditional methods and optical mapping. In: 108th ASM General Meeting. American Society for Microbiology, Boston, MA.

Becker, K., Heilmann, C., Peters, G., 2014. Coagulase-negative staphylococci. Clin. Microbiol. Rev. 27, 870–926. https://doi.org/10.1128/Cmr.00109-13.

Becker, K., van Alen, S., Idelevich, E.A., Schleimer, N., Seggewiss, J., Mellmann, A., Kaspar, U., Peters, G., 2018. Plasmid-encoded transferable *mecB*-mediated methicillin resistance in *Staphylococcus aureus*. Emerg. Infect. Dis. 24, 242–248. https://doi.org/10.3201/eid2402.171074.

Bouchami, O., Ben Hassen, A., de Lencastre, H., Miragaia, M., 2011. Molecular epidemiology of methicillin-resistant *Staphylococcus hominis* (MRSHo): low clonality and reservoirs of SCC*mec* structural elements. PLoS One 6, e21940. https://doi.org/10.1371/journal.pone.0021940.

Bouchami, O., Ben Hassen, A., de Lencastre, H., Miragaia, M., 2012. High prevalence of *mec* complex C and *ccr*C is independent of SCC*mec* type V in *Staphylococcus haemolyticus*. Eur. J. Clin. Microbiol. Infect. Dis. 31, 605–614. https://doi.org/10.1007/

s10096-011-1354-3.
Brzychczy-Wloch, M., Borszewska-Kornacka, M., Gulczynska, E., Wojkowska-Mach, J., Sulik, M., Grzebyk, M., Luchter, M., Heczko, P.B., Bulanda, M., 2013. Prevalence of antibiotic resistance in multi-drug resistant coagulase-negative staphylococci isolated from invasive infection in very low birth weight neonates in two Polish NICUs. Ann. Clin. Microb. Antimicrob. 12, 41. https://doi.org/10.1186/1476-0711-12-41.
Cavanagh, J.P., Hjerde, E., Holden, M.T.G., Kahlke, T., Klingenberg, C., Flaegstad, T., Parkhill, J., Bentley, S.D., Sollid, J.U.E., 2014. Whole-genome sequencing reveals clonal expansion of multiresistant *Staphylococcus haemolyticus* in European hospitals. J. Antimicrob. Chemother. 69, 2920–2927. https://doi.org/10.1093/jac/dku271.
Chaves, F., Garcia-Alvarez, M., Sanz, F., Alba, C., Otero, J.R., 2005. Nosocomial spread of a *Staphylococcus hominis* subsp. *novobiosepticus* strain causing sepsis in a neonatal intensive care unit. J. Clin. Microbiol. 43, 4877–4879. https://doi.org/10.1128/JCM.43.9.4877-4879.2005.
Chen, H.J., Tsai, J.C., Hung, W.C., Tseng, S.P., Hsueh, P.R., Teng, L.J., 2011. Identification of *fusB*-mediated fusidic acid resistance islands in *Staphylococcus epidermidis* isolates. Antimicrob. Agents Chemother. 55, 5842–5849. https://doi.org/10.1128/AAC.00592-11.
Chen, L.H., Zheng, D.D., Liu, B., Yang, J., Jin, Q., 2016a. VFDB 2016: hierarchical and refined dataset for big data analysis-10 years on. Nucleic Acids Res. 44, D694–D697. https://doi.org/10.1093/nar/gkv1239.
Chen, N.H., Djoko, K.Y., Veyrier, F.J., McEwan, A.G., 2016b. Formaldehyde stress responses in bacterial pathogens. Front. Microbiol. 7, 257. https://doi.org/10.3389/fmicb.2016.00257.
CLSI, 2018. Performance Standards for Antimicrobial Disk Susceptibility Tests; Approved Standard - 13th Ed. CLSI Standard M02. Clinical and Laboratory Standards Institute, Wayne, PA. https://clsi.org/standards/products/microbiology/documents/m02/.
De Bel, A., Svec, P., Petras, P., Sedlacek, I., Pantucek, R., Echahidi, F., Pierard, D., Vandamme, P., 2014. Reclassification of *Staphylococcus jettensis* De Bel et al. 2013 as *Staphylococcus petrasii* subsp. *jettensis* subsp. nov. and emended description of *Staphylococcus petrasii* Pantucek et al. 2013. Int. J. Syst. Evol. Microbiol. 64, 4198–4201. https://doi.org/10.1099/ijs.0.064758-0.
De Bel, A., Van Hoorde, K., Wybo, I., Vandoorslaer, K., Echahidi, F., De Brandt, E., Schumann, P., Ieven, M., Soetens, O., Piérard, D., Vandamme, P., 2013. *Staphylococcus jettensis* sp. nov., a coagulase-negative staphylococcal species isolated from human clinical specimens. Int. J. Syst. Evol. Microbiol. 63, 3250–3256. https://doi.org/10.1099/ijs.0.044438-0.
Deghorain, M., Bobay, L.M., Smeesters, P.R., Bousbata, S., Vermeersch, M., Perez-Morga, D., Dreze, P.A., Rocha, E.P.C., Touchon, M., Van Melderen, L., 2012. Characterization of novel phages isolated in coagulase-negative staphylococci reveals evolutionary relationships with *Staphylococcus aureus* phages. J. Bacteriol. 194, 5829–5839. https://doi.org/10.1128/Jb.01085-12.
Dhillon, B.K., Laird, M.R., Shay, J.A., Winsor, G.L., Lo, R., Nizam, F., Pereira, S.K., Waglechner, N., McArthur, A.G., Langille, M.G.I., Brinkman, F.S.L., 2015. IslandViewer 3: more flexible, interactive genomic island discovery, visualization and analysis. Nucleic Acids Res. 43, W104–W108. https://doi.org/10.1093/nar/gkv401.
Endl, J., Seidl, P.H., Fiedler, F., Schleifer, K.H., 1984. Determination of cell-wall teichoic-acid structure of staphylococci by rapid chemical and serological screening methods. Arch. Microbiol. 137, 272–280. https://doi.org/10.1007/Bf00414557.
EUCAST, 2017. Breakpoint Tables for Interpretation of MICs and Zone Diameters. The European Committee on Antimicrobial Susceptibility Testing. http://www.eucast.org/fileadmin/src/media/PDFs/EUCAST_files/Breakpoint_tables/v_7.1_Breakpoint_Tables.pdf.
Fitzgibbon, J.E., Nahvi, M.D., Dubin, D.T., John Jr., J.F., 2001. A sequence variant of *Staphylococcus hominis* with a high prevalence of oxacillin and fluoroquinolone resistance. Res. Microbiol. 152, 805–810. https://doi.org/10.1016/S0923-2508(01)01264-5.
Freiwald, A., Sauer, S., 2009. Phylogenetic classification and identification of bacteria by mass spectrometry. Nat. Protoc. 4, 732–742. https://doi.org/10.1038/nprot.2009.37.
Froggatt, J.W., Johnston, J.L., Galetto, D.W., Archer, G.L., 1989. Antimicrobial resistance in nosocomial isolates of *Staphylococcus haemolyticus*. Antimicrob. Agents Chemother. 33, 460–466. https://doi.org/10.1128/Aac.33.4.460.
Gill, S.R., Fouts, D.E., Archer, G.L., Mongodin, E.F., Deboy, R.T., Ravel, J., Paulsen, I.T., Kolonay, J.F., Brinkac, L., Beanan, M., Dodson, R.J., Daugherty, S.C., Madupu, R., Angiuoli, S.V., Durkin, A.S., Haft, D.H., Vamathevan, J., Khouri, H., Utterback, T., Lee, C., Dimitrov, G., Jiang, L., Qin, H., Weidman, J., Tran, K., Kang, K., Hance, I.R., Nelson, K.E., Fraser, C.M., 2005. Insights on evolution of virulence and resistance from the complete genome analysis of an early methicillin-resistant *Staphylococcus aureus* strain and a biofilm-producing methicillin-resistant *Staphylococcus epidermidis* strain. J. Bacteriol. 187, 2426–2438. https://doi.org/10.1128/JB.187.7.2426-2438.2005.
Hanssen, A.M., Sollid, J.U.E., 2006. SCC*mec* in staphylococci: genes on the move. FEMS Immunol. Med. Microbiol. 46, 8–20. https://doi.org/10.1111/j.1574-695X.2005.00009.x.
Harrison, E.M., Paterson, G.K., Holden, M.T., Ba, X., Rolo, J., Morgan, F.J., Pichon, B., Kearns, A., Zadoks, R.N., Peacock, S.J., Parkhill, J., Holmes, M.A., 2014. A novel hybrid SCC*mec*-*mecC* region in *Staphylococcus sciuri*. J. Antimicrob. Chemother. 69, 911–918. https://doi.org/10.1093/jac/dkt452.
Harrison, E.M., Paterson, G.K., Holden, M.T., Morgan, F.J., Larsen, A.R., Petersen, A., Leroy, S., De Vliegher, S., Perreten, V., Fox, L.K., Lam, T.J., Sampimon, O.C., Zadoks, R.N., Peacock, S.J., Parkhill, J., Holmes, M.A., 2013. A *Staphylococcus xylosus* isolate with a new *mecC* allotype. Antimicrob. Agents Chemother. 57, 1524–1528. https://doi.org/10.1128/AAC.01882-12.
Heilmann, C., Ziebuhr, W., Becker, K., 2019. Are coagulase-negative staphylococci virulent? Clin. Microbiol. Infect. 25, 1071–1080. https://doi.org/10.1016/j.cmi.2018.11.012.
Holden, M.T.G., Lindsay, J.A., Corton, C., Quail, M.A., Cockfield, J.D., Pathak, S., Batra, R., Parkhill, J., Bentley, S.D., Edgeworth, J.D., 2010. Genome sequence of a recently emerged, highly transmissible, multi-antibiotic- and antiseptic-resistant variant of methicillin-resistant *Staphylococcus aureus*, sequence type 239 (TW). J. Bacteriol. 192, 888–892. https://doi.org/10.1128/Jb.01255-09.
Ito, T., Ma, X.X., Takeuchi, F., Okuma, K., Yuzawa, H., Hiramatsu, K., 2004. Novel type V staphylococcal cassette chromosome *mec* driven by a novel cassette chromosome recombinase, *ccrC*. Antimicrob. Agents Chemother. 48, 2637–2651. https://doi.org/10.1128/AAC.48.7.2637-2651.2004.
Jia, B., Raphenya, A.R., Alcock, B., Waglechner, N., Guo, P., Tsang, K.K., Lago, B.A., Dave, B.M., Pereira, S., Sharma, A.N., Doshi, S., Courtot, M., Lo, R., Williams, L.E., Frye, J.G., Elsayegh, T., Sardar, D., Westman, E.L., Pawlowski, A.C., Johnson, T.A., Brinkman, F.S., Wright, G.D., McArthur, A.G., 2017. CARD 2017: expansion and model-centric curation of the comprehensive antibiotic resistance database. Nucleic Acids Res. 45, D566–D573. https://doi.org/10.1093/nar/gkw1004.
Joensen, K.G., Scheutz, F., Lund, O., Hasman, H., Kaas, R.S., Nielsen, E.M., Aarestrup, F.M., 2014. Real-time whole-genome sequencing for routine typing, surveillance, and outbreak detection of verotoxigenic *Escherichia coli*. J. Clin. Microbiol. 52, 1501–1510. https://doi.org/10.1128/JCM.03617-13.
Jones, P., Binns, D., Chang, H.Y., Fraser, M., Li, W.Z., McAnulla, C., McWilliam, H., Maslen, J., Mitchell, A., Nuka, G., Pesseat, S., Quinn, A.F., Sangrador-Vegas, A., Scheremetjew, M., Yong, S.Y., Lopez, R., Hunter, S., 2014. InterProScan 5: genome-scale protein function classification. Bioinformatics 30, 1236–1240. https://doi.org/10.1093/bioinformatics/btu031.
Joshi, G.S., Spontak, J.S., Klapper, D.G., Richardson, A.R., 2011. Arginine catabolic mobile element encoded *speG* abrogates the unique hypersensitivity of *Staphylococcus aureus* to exogenous polyamines. Mol. Microbiol. 82, 9–20. https://doi.org/10.1111/j.1365-2958.2011.07809.x.
Kinnevey, P.M., Shore, A.C., Brennan, G.I., Sullivan, D.J., Ehricht, R., Monecke, S., Slickers, P., Coleman, D.C., 2013. Emergence of sequence type 779 methicillin-resistant *Staphylococcus aureus* harboring a novel pseudo staphylococcal cassette chromosome *mec* (SCC*mec*)-SCC-SCC$_{CRISPR}$ composite element in Irish hospitals. Antimicrob. Agents Chemother. 57, 524–531. https://doi.org/10.1128/AAC.01689-12.
Kloos, W.E., George, C.G., Olgiate, J.S., Van Pelt, L., McKinnon, M.L., Zimmer, B.L., Muller, E., Weinstein, M.P., Mirrett, S., 1998. *Staphylococcus hominis* subsp. *novobiosepticus* subsp. nov., a novel trehalose- and *N*-acetyl-D-glucosamine-negative, novobiocin- and multiple-antibiotic-resistant subspecies isolated from human blood cultures. Int. J. Syst. Bacteriol. 48, 799–812. https://doi.org/10.1099/00207713-48-3-799.
Kumar, S., Stecher, G., Tamura, K., 2016. MEGA7: molecular evolutionary genetics analysis version 7.0 for bigger datasets. Mol. Biol. Evol. 33, 1870–1874. https://doi.org/10.1093/molbev/msw054.
Kuntova, L., Pantucek, R., Rajova, J., Ruzickova, V., Petras, P., Maslanova, I., Doskar, J., 2012. Characteristics and distribution of plasmids in a clonally diverse set of methicillin-resistant *Staphylococcus aureus* strains. Arch. Microbiol. 194, 607–614. https://doi.org/10.1007/s00203-012-0797-y.
Lee, I., Ouk Kim, Y., Park, S.C., Chun, J., 2016. OrthoANI: an improved algorithm and software for calculating average nucleotide identity. Int. J. Syst. Evol. Microbiol. 66, 1100–1103. https://doi.org/10.1099/ijsem.0.000760.
Li, M., Du, X., Villaruz, A.E., Diep, B.A., Wang, D.C., Song, Y., Tian, Y.R., Hu, J.H., Yu, F.Y., Lu, Y., Otto, M., 2012. MRSA epidemic linked to a quickly spreading colonization and virulence determinant. Nat. Med. 18, 816–819. https://doi.org/10.1038/nm.2692.
Li, S., Skov, R.L., Han, X., Larsen, A.R., Larsen, J., Sorum, M., Wulf, M., Voss, A., Hiramatsu, K., Ito, T., 2011. Novel types of staphylococcal cassette chromosome mec elements identified in clonal complex 398 methicillin-resistant *Staphylococcus aureus* strains. Antimicrob. Agents Chemother. 55, 3046–3050. https://doi.org/10.1128/AAC.01475-10.
Liu, P., Peng, F., Hu, Q., Tang, Y., Kang, H., Tong, T., 2018. The induction, purification, whole genome sequencing and comparative genome analysis of a novel *Staphylococcus haemolyticus* bacteriophage IME-SA4. J. Chin. Phys. 20, 546–550. https://doi.org/10.3760/cma.j.issn.1008-1372.2018.04.018.
Lopes, A., Tavares, P., Petit, M.A., Guerois, R., Zinn-Justin, S., 2014. Automated classification of tailed bacteriophages according to their neck organization. BMC Genomics 15, 1027. https://doi.org/10.1186/1471-2164-15-1027.
Maslanova, I., Doskar, J., Varga, M., Kuntova, L., Muzik, J., Maluskova, D., Ruzickova, V., Pantucek, R., 2013. Bacteriophages of *Staphylococcus aureus* efficiently package various bacterial genes and mobile genetic elements including SCC*mec* with different frequencies. Environ. Microbiol. Rep. 5, 66–73. https://doi.org/10.1111/j.1758-2229.2012.00378.x.
McCallum, N., Brassinga, A.K.C., Sifri, C.D., Berger-Bächi, B., 2007. Functional characterization of TcaA: minimal requirement for teicoplanin susceptibility and role in *Caenorhabditis elegans* virulence. Antimicrob. Agents Chemother. 51, 3836–3843. https://doi.org/10.1128/AAC.00722-07.
Meier-Kolthoff, J.P., Auch, A.F., Klenk, H.P., Goker, M., 2013. Genome sequence-based species delimitation with confidence intervals and improved distance functions. BMC Bioinformatics 14, 60. https://doi.org/10.1186/1471-2105-14-60.
Mellmann, A., Becker, K., von Eiff, C., Keckevoet, U., Schumann, P., Harmsen, D., 2006. Sequencing and staphylococci identification. Emerg. Infect. Dis. 12, 333–336. https://doi.org/10.3201/eid1202.050962.
Morozov, G.I., Porat, N., Kushnir, T., Najmuldeen, H., Adawi, A., Chalifa-Caspi, V., Benisty, R., Ohayon, A., Liron, O., Azriel, S., Malka, I., Dotan, S., Portnoi, M., Piotrowski, A.A., Kafka, D., Hajaj, B., Fishilevich, T., Shagan, M., Tal, M., Ellis, R., Morrison, D.A., Mitchell, A.M., Mitchell, T.J., Dagan, R., Yesilkaya, H., Nebenzahl, Y.M., 2018. Flavin reductase contributes to pneumococcal virulence by protecting

from oxidative stress and mediating adhesion and elicits protection against pneumococcal challenge. Sci. Rep. 8, 314. https://doi.org/10.1038/s41598-017-18645-8.
Novick, R.P., 1990. Molecular Biology of the Staphylococci. VCH Publishers, New York.
Nurk, S., Bankevich, A., Antipov, D., Gurevich, A.A., Korobeynikov, A., Lapidus, A., Prjibelski, A.D., Pyshkin, A., Sirotkin, A., Sirotkin, Y., Stepanauskas, R., Clingenpeel, S.R., Woyke, T., McLean, J.S., Lasken, R., Tesler, G., Alekseyev, M.A., Pevzner, P.A., 2013. Assembling single-cell genomes and mini-metagenomes from chimeric MDA products. J. Comput. Biol. 20, 714–737. https://doi.org/10.1089/cmb.2013.0084.
Okonechnikov, K., Golosova, O., Fursov, M., UGENE team, 2012. Unipro UGENE: a unified bioinformatics toolkit. Bioinformatics 28, 1166–1167. https://doi.org/10.1093/bioinformatics/bts091.
Otto, M., 2013. Coagulase-negative staphylococci as reservoirs of genes facilitating MRSA infection: staphylococcal commensal species such as *Staphylococcus epidermidis* are being recognized as important sources of genes promoting MRSA colonization and virulence. Bioessays 35, 4–11. https://doi.org/10.1002/bies.201200112.
Panda, S., Kar, S., Sharma, S., Singh, D.V., 2016. Multidrug-resistant *Staphylococcus haemolyticus* isolates from infected eyes and healthy conjunctivae in India. J. Glob. Antimicrob. Resist. 6, 154–159. https://doi.org/10.1016/j.jgar.2016.05.006.
Panda, S., Singh, D.V., 2018. Biofilm formation by ica-negative ocular isolates of *Staphylococcus haemolyticus*. Front. Microbiol. 9, 2687. https://doi.org/10.3389/fmicb.2018.02687.
Pantucek, R., Gotz, F., Doskar, J., Rosypal, S., 1996. Genomic variability of *Staphylococcus aureus* and the other coagulase-positive *Staphylococcus* species estimated by macrorestriction analysis using pulsed-field gel electrophoresis. Int. J. Syst. Bacteriol. 46, 216–222. https://doi.org/10.1099/00207713-46-1-216.
Pantucek, R., Sedlacek, I., Indrakova, A., Vrbovska, V., Maslanova, I., Kovarovic, V., Svec, P., Kralova, S., Kristofova, L., Keklakova, J., Petras, P., Doskar, J., 2018. *Staphylococcus edaphicus* sp. nov., isolated in Antarctica, harbors the *mec*C gene and genomic islands with a suspected role in adaptation to extreme environments. Appl. Environ. Microbiol. 84, e01746–17. https://doi.org/10.1128/AEM.01746-17.
Pantucek, R., Svec, P., Dajcs, J.J., Machova, I., Cernohlavkova, J., Sedo, O., Gelbicova, T., Maslanova, I., Doskar, J., Zdrahal, Z., Ruzickova, V., Sedlacek, I., 2013. *Staphylococcus petrasii*sp. nov. including *S. petrasii* subsp. *petrasii* subsp. nov. and *S. petrasii* subsp. *croceilyticus* subsp. nov., isolated from human clinical specimens and human ear infections. Syst. Appl. Microbiol. 36, 90–95. https://doi.org/10.1016/j.syapm.2012.11.004.
Pulverer, G., Pillich, J., Klein, A., Krivankova, M., 1974. Studies on lysogeny of *Staphylococcus albus*. Med. Microbiol. Immunol. 159, 115–119. https://doi.org/10.1007/BF02123723.
Rissman, A.I., Mau, B., Biehl, B.S., Darling, A.E., Glasner, J.D., Perna, N.T., 2009. Reordering contigs of draft genomes using the Mauve aligner. Bioinformatics 25, 2071–2073. https://doi.org/10.1093/bioinformatics/btp356.
Rossi, C.C., Souza-Silva, T., Araujo-Alves, A.V., Giambiagi-deMarval, M., 2017. CRISPR-Cas systems features and the gene-reservoir role of coagulase-negative staphylococci. Front. Microbiol. 8, 1545. https://doi.org/10.3389/fmicb.2017.01545.
Sadaka, A., Palmer, K., Suzuki, T., Gilmore, M.S., 2014. *In vitro* and *in vivo* models of *Staphylococcus aureus* endophthalmitis implicate specific nutrients in ocular infection. PLoS One 9, e110872. https://doi.org/10.1371/journal.pone.0110872.
Siebold, C., Flukiger, K., Beutler, R., Erni, B., 2001. Carbohydrate transporters of the bacterial phosphoenolpyruvate: sugar phosphotransferase system (PTS). FEBS Lett. 504, 104–111. https://doi.org/10.1016/S0014-5793(01)02705-3.
Siguier, P., Perochon, J., Lestrade, L., Mahillon, J., Chandler, M., 2006. ISfinder: the reference centre for bacterial insertion sequences. Nucleic Acids Res. 34, D32–D36. https://doi.org/10.1093/nar/gkj014.
Stegger, M., Andersen, P.S., Kearns, A., Pichon, B., Holmes, M.A., Edwards, G., Laurent, F., Teale, C., Skov, R., Larsen, A.R., 2012. Rapid detection, differentiation and typing of methicillin-resistant *Staphylococcus aureus* harbouring either *mecA* or the new *mecA* homologue $mecA_{LGA251}$. Clin. Microbiol. Infect. 18, 395–400. https://doi.org/10.1111/j.1469-0691.2011.03715.x.
Svec, P., De Bel, A., Sedlacek, I., Petras, P., Gelbicova, T., Cernohlavkova, J., Maslanova, I., Cnockaert, M., Varbanovova, I., Echahidi, F., Vandamme, P., Pantucek, R., 2015. *Staphylococcus petrasii* subsp. *pragensis* subsp. nov., occurring in human clinical material. Int. J. Syst. Evol. Microbiol. 65, 2071–2077. https://doi.org/10.1099/ijs.0.000220.
Svec, P., Pantucek, R., Petras, P., Sedlacek, I., Novakova, D., 2010. Identification of *Staphylococcus* spp. using $(GTG)_5$-PCR fingerprinting. Syst. Appl. Microbiol. 33, 451–456. https://doi.org/10.1016/j.syapm.2010.09.004.
Takeuchi, F., Watanabe, S., Baba, T., Yuzawa, H., Ito, T., Morimoto, Y., Kuroda, M., Cui, L.Z., Takahashi, M., Ankai, A., Baba, S., Fukui, S., Lee, J.C., Hiramatsu, K., 2005. Whole-genome sequencing of *Staphylococcus haemolyticus* uncovers the extreme plasticity of its genome and the evolution of human-colonizing staphylococcal species. J. Bacteriol. 187, 7292–7308. https://doi.org/10.1128/Jb.187.21.7292-7308.2005.
Truong-Bolduc, Q.C., Bolduc, G.R., Okumura, R., Celino, B., Bevis, J., Liao, C.H., Hooper, D.C., 2011. Implication of the NorB efflux pump in the adaptation of *Staphylococcus aureus* to growth at acid pH and in resistance to moxifloxacin. Antimicrob. Agents Chemother. 55, 3214–3219. https://doi.org/10.1128/AAC.00289-11.
Wang, Y., Coleman-Derr, D., Chen, G.P., Gu, Y.Q., 2015. OrthoVenn: a web server for genome wide comparison and annotation of orthologous clusters across multiple species. Nucleic Acids Res. 43, W78–W84. https://doi.org/10.1093/nar/gkv487.
Werbick, C., Becker, K., Mellmann, A., Juuti, K.M., von Eiff, C., Peters, G., Kuusela, P.I., Friedrich, A.W., Sinha, B., 2007. Staphylococcal chromosomal cassette *mec* type I, *spa* type, and expression of Pls are determinants of reduced cellular invasiveness of methicillin-resistant *Staphylococcus aureus* isolates. J. Infect. Dis. 195, 1678–1685. https://doi.org/10.1086/517517.
Wick, R.R., Schultz, M.B., Zobel, J., Holt, K.E., 2015. Bandage: interactive visualization of *de novo* genome assemblies. Bioinformatics 31, 3350–3352. https://doi.org/10.1093/bioinformatics/btv383.
Wilson, L.K., Coombs, G.W., Christiansen, K., Grubb, W.B., O'Brien, F.G., 2016. Characterization of a novel staphylococcal cassette chromosome composite island from community-associated MRSA isolated in aged care facilities in Western Australia. J. Antimicrob. Chemother. 71, 3372–3375. https://doi.org/10.1093/jac/dkw317.
Winstel, V., Liang, C., Sanchez-Carballo, P., Steglich, M., Munar, M., Broker, B.M., Penades, J.R., Nubel, U., Holst, O., Dandekar, T., Peschel, A., Xia, G., 2013. Wall teichoic acid structure governs horizontal gene transfer between major bacterial pathogens. Nat. Commun. 4, 2345. https://doi.org/10.1038/ncomms3345.
Wu, S.W., de Lencastre, H., Tomasz, A., 1998. Genetic organization of the *mec*A region in methicillin-susceptible and methicillin-resistant strains of *Staphylococcus sciuri*. J. Bacteriol. 180, 236–242.
Yu, D., Pi, B., Chen, Y., Wang, Y., Ruan, Z., Otto, M., Yu, Y., 2014. Characterization of the staphylococcal cassette chromosome composite island of *Staphylococcus haemolyticus* SH32, a methicillin-resistant clinical isolate from China. PLoS One 9, e87346. https://doi.org/10.1371/journal.pone.0087346.
Yu, W.Q., Kim, H.K., Rauch, S., Schneewind, O., Missiakas, D., 2017. Pathogenic conversion of coagulase-negative staphylococci. Microbes Infect. 19, 101–109. https://doi.org/10.1016/j.micinf.2016.12.002.
Zankari, E., Hasman, H., Cosentino, S., Vestergaard, M., Rasmussen, S., Lund, O., Aarestrup, F.M., Larsen, M.V., 2012. Identification of acquired antimicrobial resistance genes. J. Antimicrob. Chemother. 67, 2640–2644. https://doi.org/10.1093/jac/dks261.
Zeman, M., Maslanova, I., Indrakova, A., Siborova, M., Mikulasek, K., Bendickova, K., Plevka, P., Vrbovska, V., Zdrahal, Z., Doskar, J., Pantucek, R., 2017. *Staphylococcus sciuri* bacteriophages double-convert for staphylokinase and phospholipase, mediate interspecies plasmid transduction, and package *mec*A gene. Sci. Rep. 7, 46319. https://doi.org/10.1038/srep46319.
Zhai, Y., He, Z., Kang, Y., Yu, H., Wang, J., Du, P., Zhang, Z., Hu, S., Gao, Z., 2016. Complete nucleotide sequence of pH11, an IncHI2 plasmid conferring multi-antibiotic resistance and multi-heavy metal resistance genes in a clinical *Klebsiella pneumoniae* isolate. Plasmid 86, 26–31. https://doi.org/10.1016/j.plasmid.2016.04.001.
Zhang, Q., Ye, Y., 2017. Not all predicted CRISPR-Cas systems are equal: isolated *cas* genes and classes of CRISPR like elements. BMC Bioinformatics 18, 92. https://doi.org/10.1186/s12859-017-1512-4.
Zong, Z.Y., Peng, C.H., Lu, X.J., 2011. Diversity of SCC*mec* elements in methicillin-resistant coagulase-negative staphylococci clinical isolates. PLoS One 6, e20191. https://doi.org/10.1371/journal.pone.0020191.
Zuniga, M., Comas, I., Linaje, R., Monedero, V., Yebra, M.J., Esteban, C.D., Deutscher, J., Perez-Martinez, G., Gonzalez-Candelas, F., 2005. Horizontal gene transfer in the molecular evolution of mannose PTS transporters. Mol. Biol. Evol. 22, 1673–1685. https://doi.org/10.1093/molbev/msi163.